AGU ADVANCING EARTH AND SPACE SCIENCES

Geophysical Research Letters

RESEARCH LETTER
10.1029/2024GL110520

Precession-Driven Variations in the Indonesian Throughflow Thermocline and Its Implications on the Agulhas Leakage

Peng Zhang[1], Jian Xu[1], Ann Holbourn[2], Wolfgang Kuhnt[2], Renjie Pei[2,3], Zhifang Xiong[4], and Tiegang Li[4]

[1]State Key Laboratory of Continental Dynamics, Department of Geology, Northwest University, Xi'an, China, [2]Institute of Geosciences, Christian-Albrechts-University, Kiel, Germany, [3]Department of Geological Sciences, San Diego State University, San Diego, CA, USA, [4]Key Laboratory of Marine Geology and Metallogeny, First Institute of Oceanography, Ministry of Natural Resources, Qingdao, China

Key Points:

- Precession drove variations in the ITF thermocline by modulating the intensity of the Australian-Indonesian winter monsoon, ENSO-like states and formation of the North Pacific Tropical Water
- Variations in the ITF thermocline regulated the amount of AL and seawater temperature and salinity of South Atlantic thermocline

Supporting Information:

Supporting Information may be found in the online version of this article.

Correspondence to:

J. Xu,
jx08@live.cn

Citation:

Zhang, P., Xu, J., Holbourn, A., Kuhnt, W., Pei, R., Xiong, Z., & Li, T. (2024). Precession-driven variations in the Indonesian throughflow thermocline and its implications on the Agulhas leakage. *Geophysical Research Letters*, *51*, e2024GL110520. https://doi.org/10.1029/2024GL110520

Received 29 MAY 2024
Accepted 12 SEP 2024

Abstract

The Indonesian Throughflow (ITF) thermocline, as exclusive water source for the "warm water route" of the Atlantic Meridional Overturning Circulation (AMOC), provides waters that exit the Indian Ocean and join the AMOC upper limb via the Agulhas Leakage (AL). Hence, investigating long-term variations in the ITF thermocline and its implications on the AL is important for understanding dynamics of the AMOC. Here, the thermohaline history of the ITF thermocline was reconstructed for the last ~410 kyr based on $\delta^{18}O$ and Mg/Ca of planktonic foraminifera from International Ocean Discovery Program Site U1483. By integrating the new and published records, we found that precession drives variation of the ITF thermocline through modulating the intensity of the Australian-Indonesian winter monsoon, El Niño-Southern Oscillation-like states and formation of the North Pacific Tropical Water, in turn exerting a transoceanic influence on the amount of the AL and seawater temperature and salinity of the South Atlantic thermocline.

Plain Language Summary

It is widely acknowledged that the Indonesian Throughflow (ITF), a key component of the global thermohaline circulation, plays an important role in the global climate and ocean circulation. However, in contrast to concentrating on the factors that shaped the ITF in the geological history, few studies considered the ITF as a factor to influence climate and ocean circulation, especially on long timescales. In this study, we utilized shell $\delta^{18}O$ and Mg/Ca of a planktonic foraminiferal thermocline-dwelling species from the Timor Sea, the main outflow passage of the ITF, to reconstruct the temperature and salinity changes of the ITF thermocline during the past ~410 kyr. By integrating the new and published paleo-oceanographic and -climatological records, we found that the ~20-kyr wobbles of the Earth's axis (precession) induced variations in the flow strength and seawater temperature and salinity of the ITF thermocline, and in turn regulated the amount of the Agulhas Leakage and seawater temperature and salinity of the South Atlantic thermocline. Our results underscore the essential role of the ITF in the connectivity among the oceans.

1. Introduction

The Indonesian Throughflow (ITF) represents a flow of Pacific waters through the Indonesian archipelagos into the Indian Ocean under the effect of pressure gradient between the Pacific and Indian Ocean (Cresswell et al., 1993; Gordon, 2005) (Figure 1). As the solo conduit between the two oceans, the ITF comprises the key component of the global thermohaline circulation at low latitudes. It regulates not only the heat and freshwater budgets between the Pacific and Indian Ocean but also the thermohaline distribution between the low- and high-latitudes, and thus plays an important role in shaping the regional and global climate (Gordon, 1986, 2005).

ITF waters are principally derived from the North Pacific thermocline, and the dominant transport of the ITF occurs in the thermocline (Gordon & Fine, 1996; Sprintall et al., 2009). Almost half of ITF thermocline water enters the Indian Ocean through the Timor Passage, while the rest flows through the Lombok and Ombai Straits (Gordon, 2005) (Figure 1). Subsequently, the thermocline water joins in the so-called "warm water route" of the Atlantic Meridional Overturning Circulation (AMOC) that tracks from the Indian Ocean to the Atlantic through the Agulhas leakage (AL) (Gordon, 1985, 1986; Rühs et al., 2019). Haines et al. (1999) and Song et al. (2004) suggested that ~90% of the ITF thermocline water exits the Indian Ocean via the AL. Meanwhile, Durgadoo et al. (2017) also pointed to that almost half of the AL water originates from ITF thermocline.

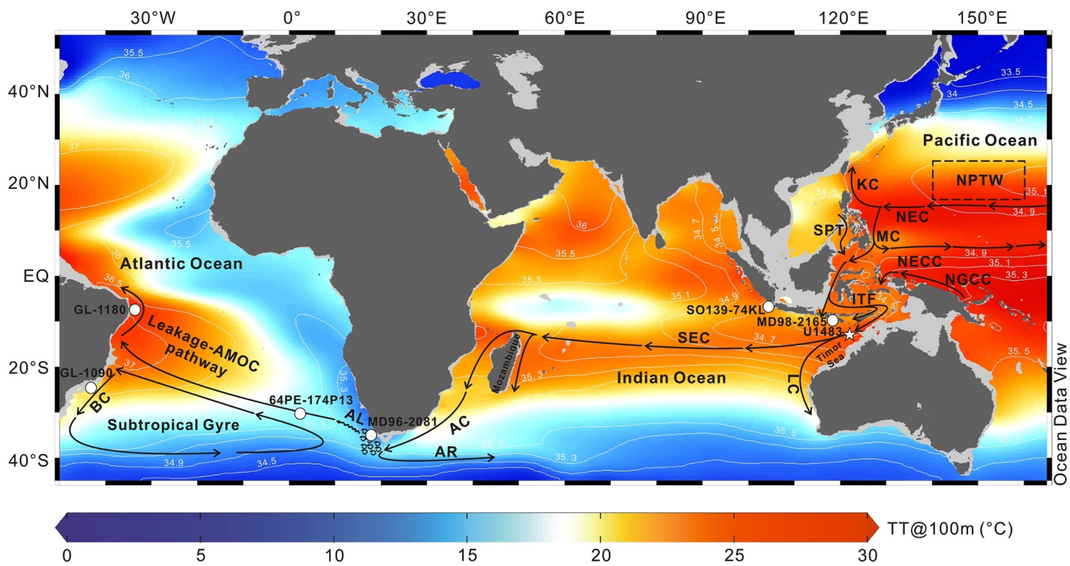

Figure 1. The distribution of annual mean TT and TS (Locarnini et al., 2024; Reagan et al., 2024) and ocean currents in the Pacific, Indian and Atlantic Oceans (Beal et al., 2011; Gordon et al., 2010, 2012; Li et al., 2020). White filled star marks Site U1483 (this study). White filled circles mark reference cores. NEC, North Equatorial Current; KC, Kuroshio Current; MC, Mindanao Current; NECC, North Equatorial Countercurrent; NGCC, New Guinea Coastal Current; LC, Leeuwin Current; AR, Agulhas retroflection; BC, Brazil Current. Gray-shaded areas denote exposed shelf areas with the sea level drop 100 m. The dotted box denotes the formation region of NPTW.

The AL mainly enters the South Atlantic as thermocline water by spreading of rings (Donners & Drijfhout, 2004; de Ruijter et al., 1999) (Figure 1). The leakage contributes to the South Atlantic Central Water, which fills mostly at depths of 100–600 m, and influences thermocline seawater temperature and salinity in the South Atlantic (Ballalai et al., 2019; Donners & Drijfhout, 2004; Peterson & Stramma, 1991; de Ruijter et al., 1999). Previous studies suggested that the AL is a key component of the global thermohaline circulation. This is because it feeds warm and saline waters into the upper arm of the AMOC, with a significant portion originating from the ITF thermocline. This in turn regulates the variability and strength of the AMOC (Durgadoo et al., 2017; Gordon, 1986). It is thus that investigating the impact of the ITF thermocline on the AL is useful for understanding the link between low- and high-latitudes, which may provide insightful perspectives into the low-latitude forcing on the global climate. This study presents new profiles of ITF thermocline temperature (TT) and salinity (TS) spanning the past ~410 kyr from International Ocean Discovery Program (IODP) Site U1483, which situates in the main outflow passage of the ITF in the Timor Sea (Figure 1). Thermocline water flowing over this site are supposed to be eventually advected to the AL by the "warm water route" (Gordon, 1986). Our purpose is to decipher long-term variations of the ITF thermocline on orbital timescales and its potential implications on the AL.

2. Materials and Methods

IODP Site U1483 (13.09°S, 121.80°E; water depth: 1,733 m) was recovered at the Timor Sea (Figure 1; Rosenthal et al., 2017). Sediments from this site were sampled at ~20 cm intervals along the revised SPLICE from 0 to 4,100 cm composite depth scale (Zhang et al., 2020). The preliminary age model of the sediment succession was established by directly tuning the benthic $\delta^{18}O$ to the LR04 stack (Zhang et al., 2020). The age model was later improved by correlation of XRF-derived ln (K/Ca) record from Site U1483 to Core MD01-2378, which has a robust age model based on AMS^{14}C dates and the correlation of benthic $\delta^{18}O$ to the LR04 stack (Zhang et al., 2020). This sediment succession tracks the hydrological history of ITF thermocline over the past ~410 kyr with a temporal resolution of ~2 kyr.

Approximately 35 tests of planktonic foraminifera *Pulleniatina obliquiloculata*, recording the annual mean thermocline (70–125 m) conditions in the Timor Sea (Zhang et al., 2019), were selected from the size fraction of 250 to 315 μm for paired Mg/Ca and $\delta^{18}O$ analysis. All tests were lightly crushed, homogeneously mixed and visually split into three aliquots. Two aliquots were cleaned with a reductive step following the procedures from Rosenthal et al. (1997), Martin and Lea (2002) and Barker et al. (2003) and were analyzed for Mg/Ca ratios on a Spectro Ciros SOP CCD inductively coupled plasma optical emission spectrometer (ICP-OES) in Institute of Geosciences at Kiel University. In order to monitor the measurement quality and machine drift, the certified reference material ECRM 752-1 (Greaves et al., 2008) was analyzed after every sixth sample. The non-linear correlation of Fe/Ca, Al/Ca and Mn/Ca with Mg/Ca indicates a good cleaning efficacy that effectively removed contaminations (Figure S1 in Supporting Information S1). The average reproducibility of Mg/Ca is ±0.13 mmol/mol based on the measurement of 20 replicate samples. Previous studies indicated that salinity has negligible influence on planktonic foraminiferal Mg/Ca in the Timor Sea and we thus did not correct for salinity effects (Gray & Evans, 2019; Zhang et al., 2019). As suggested by Xu et al. (2010), we used the species-specific calibrated equation $T = \ln(\mathrm{Mg/Ca}/0.328)/0.09$ (Anand et al., 2003) to convert Mg/Ca ratios into TT. The other aliquot of foraminiferal tests was cleaned and measured for $\delta^{18}O$ with a Finnigan MAT 253 mass spectrometer coupled to a Kiel-Carbo IV device in Leibniz Laboratory of Kiel University. Based on the performance of international and laboratory-internal standard carbonates, the precision is better than ±0.09‰. The results were calibrated using the National Bureau of Standard (NBS) 19 and reported on the Vienna Pee Dee Belemnite (VPDB) scale. The average reproducibility of $\delta^{18}O$ is ±0.12‰ based on the same 20 replicate samples as for Mg/Ca reproducibility. Local thermocline seawater $\delta^{18}O$ ($\delta^{18}O_{sw\text{-}c}$) was calculated from the $\delta^{18}O$ of *P. obliquiloculata* after removing the effects of calcification temperature and global ice volume (Bemis et al., 1998; Hut, 1987). The global ice volume curve of Spratt and Lisiecki (2016), that is also based on the LR04 chronology, was used for ice-volume correction for purpose of maintaining chronological consistency and removing ice-volume induced precession signals from the $\delta^{18}O_{sw\text{-}c}$ record. Calculated uncertainties (1σ) of ITF thermocline temperature and $\delta^{18}O_{sw\text{-}c}$ are ∼1°C and ∼0.25‰ based on the method from Mohtadi et al. (2014). In this study, cross-spectral analysis was performed by Redfit-X with rectangular window (Ólafsdóttir et al., 2016), which shows the phase relationship and Monte Carlo 95% confidence interval between two timeseries. Spectral analysis was performed using REDFIT with a rectangular window (Schulz & Mudelsee, 2002), which shows the red noise and 90% and 95% confidence intervals of timeseries. Bandpass filtering was carried out by the Fast Fourier transform from the Origin software package.

3. Results and Discussion

3.1. Variations in the ITF Thermocline and the Influencing Factors

Pulleniatina obliquiloculata $\delta^{18}O$ of Site U1483 varies between −1.6‰ and −0.16‰ over the past ∼410 kyr and exhibits obvious glacial-interglacial contrasts (Figure S2a in Supporting Information S1). *Pulleniatina obliquiloculata* Mg/Ca varies between 1.73 and 3.04 mmol/mol, equal to TT changes of 18.5°C–25.7°C (Figure S2b in Supporting Information S1). The average Mg/Ca-based TT during the Holocene is 22.1°C, this is close to the modern annual mean TT of 22.4°C at Site U1483 (Locarnini et al., 2024). Thermocline $\delta^{18}O_{sw\text{-}c}$ varies between −0.48 and 0.97‰ (Figure S2c in Supporting Information S1). Spectral analysis indicates that thermocline temperature and $\delta^{18}O_{sw\text{-}c}$ at Site U1483 over the past ∼410 kyr are merely dominated by precessional cycles (Figures S3a and S3b in Supporting Information S1). Precessional cyclicities in thermocline profiles have also been recorded in Core SO18480 nearby Site U1483 (Jian et al., 2022).

Cross-spectral analysis shows that Site U1483TT and precession are significantly coherent during the past ∼410 kyr and TT maxima lag precession minima only by ∼26° or ∼1.66 kyr (Figures S3h and S3i in Supporting Information S1), indicating that high (low) TT was tied to precession minima (maxima). Thermocline $\delta^{18}O_{sw\text{-}c}$ in the Timor Sea could be used to trace changes in the TS with enriched (depleted) $\delta^{18}O_{sw\text{-}c}$ denoting high (low) TS (Holbourn et al., 2011). Similarly, Site U1483 thermocline $\delta^{18}O_{sw\text{-}c}$ is also strongly correlated to precession (Figures S3h and S3i in Supporting Information S1). The phase difference between Site U1483 thermocline $\delta^{18}O_{sw\text{-}c}$ maxima and precession minima is also ∼26° (Figures S3h and S3i in Supporting Information S1), indicating that high (low) TS happened in consistence with precession minima (maxima) during the last ∼410 kyr (Figures S3h and S3i in Supporting Information S1). The TT difference between Cores MD98-2165 and SO139-74KL (ΔTT) (Figure 1), as a proxy of the ITF strength with large values denoting increased transport of the ITF thermocline and vice versa, also significantly fluctuated on the precession band (Figure S3c in Supporting Information S1) (see details in Pang et al. (2021)). The ΔTT is highly coherent with precession, the ΔTT maxima lagging precession minima by ∼32° or ∼2.04 kyr (Figures S3h and S3i in Supporting Information S1), indicating that increased (decreased) transport of the ITF thermocline occurred during precession minima (maxima). The robust visual phase coherence of precession-bandpass filters of the proxy records with the precession parameter demonstrates the above findings that high (low) TT and TS and increased (decreased) transport of the ITF thermocline coincide with precession minima (maxima), suggesting that precession may be the main driving force for the variations in the ITF thermocline during the past ~410 kyr (Figures 2a, and 2d–2f).

Previous studies disclosed that precession could directly influence the ITF thermocline by regulating air-sea processes in low latitudes such as intensity of the Australian-Indonesian winter monsoon (AIWM), state of El Niño-Southern Oscillation (ENSO) and formation of the North Pacific Tropical Water (NPTW) (e.g., Pang et al., 2021; Zhang et al., 2018, 2021). Core SO139-74KL revealed that the total organic carbon (TOC) content, a proxy of the AIWM intensity, was dominated by precession band variance (Figure S3d in Supporting Information S1) (Lückge et al., 2009). It seems that greater (lesser) heating of the Asian continent enhanced (reduced) the atmospheric pressure gradient between Asian and Australian continents during precession minima (maxima) or boreal summer insolation maxima (minima), leading to enhanced (weakened) AIWM (Figures 2a and 2c) (Lückge et al., 2009). Modern observations suggested that the maximum transport of the ITF occurs during the AIWM, bringing more warm and saline water from the western tropical Pacific to the Indonesian seas (Gordon, 2005; Gordon et al., 2012; Sprintall et al., 2009). Thus, the increased transport of the ITF when the AIWM enhanced during the precession minima would lead to raised TT and TS in the Timor Sea (Figures 2a, 2c, and 2d–2f) (Pang et al., 2021), and vice versa.

Model studies demonstrated that precession regulates the ENSO-like conditions on orbital timescales (Clement & Cane, 1999; Clement et al., 1999; Shi et al., 2012). A possible regulating mechanism is that the decreased average sea surface temperature from December to February in the Niño3.4 region during the low precession would lead to a La Niña-like state and reversely the increased average sea surface temperature during the high precession to an El Niño-like state (Figures 2a and 2b) (Shi et al., 2012). Moreover, modern observation shows that freshwater plug (~upper 100 m waters) disappears in the northern Makassar Strait when the Sibutu Passage Throughflow (SPT) is undeveloped, in addition to the increased pressure gradient between the western tropical Pacific and Indian Ocean, allowing injection of western tropical Pacific warm and saline upper waters into the Indonesian seas during La Niña events (Gordon, 2005; Gordon et al., 2012). As a result, high TT and TS appear in the Timor Sea along with increased transport of the ITF thermocline (Ffield et al., 2000; Gordon et al., 2012). The opposite situation occurs during El Niño events. The La Niña/El Niño-like episodes in the past during precession minima/maxima should be analogs to the modern observations (Figures 2a, 2b, and 2d–2f).

It is worthy of noting that formation of the NPTW could be closely correlated to precession (Dang et al., 2012; Zhang et al., 2018). Increased (decreased) boreal summer insolation causes stronger (weaker) evaporation in the North Pacific during the low (high) precession. Formation of the NPTW could be ascribed to evaporation over precipitation in the North Pacific, resulting in increased sea surface salinity, which induces sinking of the surface water down to a water depth of 50–300 m (Cannon, 1966; Fine et al., 1994, 2001; Tsuchiya, 1968). These waters are subsequently advected into the ITF thermocline (Fine et al., 1994; Gordon, 1986). Under this circumstance, the temperature and salinity and the amount of the NPTW are effectively controlled by boreal summer insolation. In details, the temperature and salinity raise and the amount of the NPTW increases during increased boreal summer insolation, and vice versa. ITF waters are principally derived from the North Pacific thermocline (Gordon & Fine, 1996; Sprintall et al., 2009). It is thus indicated that more (less) NPTW with high (low) temperature and salinity into the ITF thermocline during the low (high) precession, leading to increased (decreased) transport of the ITF thermocline and high (low) TT and TS (Figures 2a, and 2d–2f). In summary, our results suggest that precession might drive variations of the ITF thermocline through modulating the intensity of the AIWM, ENSO-like states and formation of the NPTW over the past ~410 kyr (Figure 4).

3.2. Implications of ITF Thermocline on the AL

The relative abundance of Agulhas leakage fauna (ALF (%)) from Core MD96-2081 was used as a foraminiferal proxy to estimate the amount of the AL (Peeters et al., 2004). Spectral analysis shows that ALF (%) displays significant precession cycles, indicating dominance of precession on the AL (Figure S3e in Supporting Information S1). Furthermore, ALF (%) and precession are highly coherent and ALF (%) maxima lag precession minima only by ~24° or ~1.53 kyr (Figures S3h and S3i in Supporting Information S1), pointing to concurrence of the strong (weak) AL and precession minima (maxima). This finding is supported by the in-phase variation

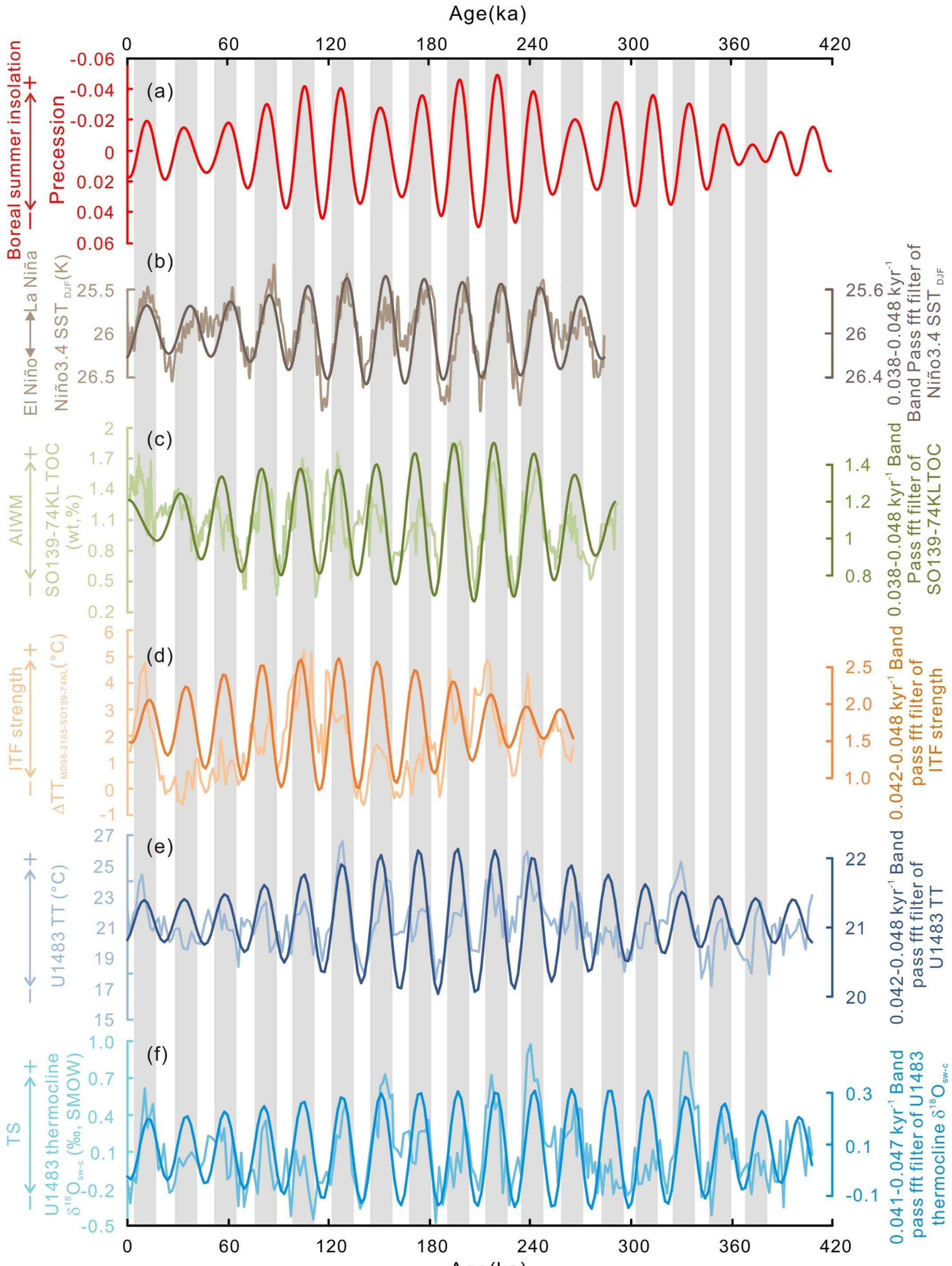

Figure 2. Comparison of variability in the temperature, salinity and strength of the ITF thermocline with the ENSO-like states and the intensity of Australian-Indonesian winter monsoon (AIWM) on the precession band. (a) Precession parameter (Berger & Loutre, 1991); (b) Average sea surface temperature from December to February in the Niño3.4 region (Niño3.4 SST_{DJF}) as a proxy for the ENSO-like states (Shi et al., 2012); (c) TOC content from Core SO139-74KL as a proxy for the AIWM intensity (Lückge et al., 2009); (d) $\Delta TT_{MD98\text{-}2165\text{-}SO139\text{-}74KL}$ as a proxy for the ITF strength (Pang et al., 2021); (e) TT and (f) TS from Site U1483 (this study). In panels (c–f), superimposed on the raw data curves are precession bandpass filtering curves.

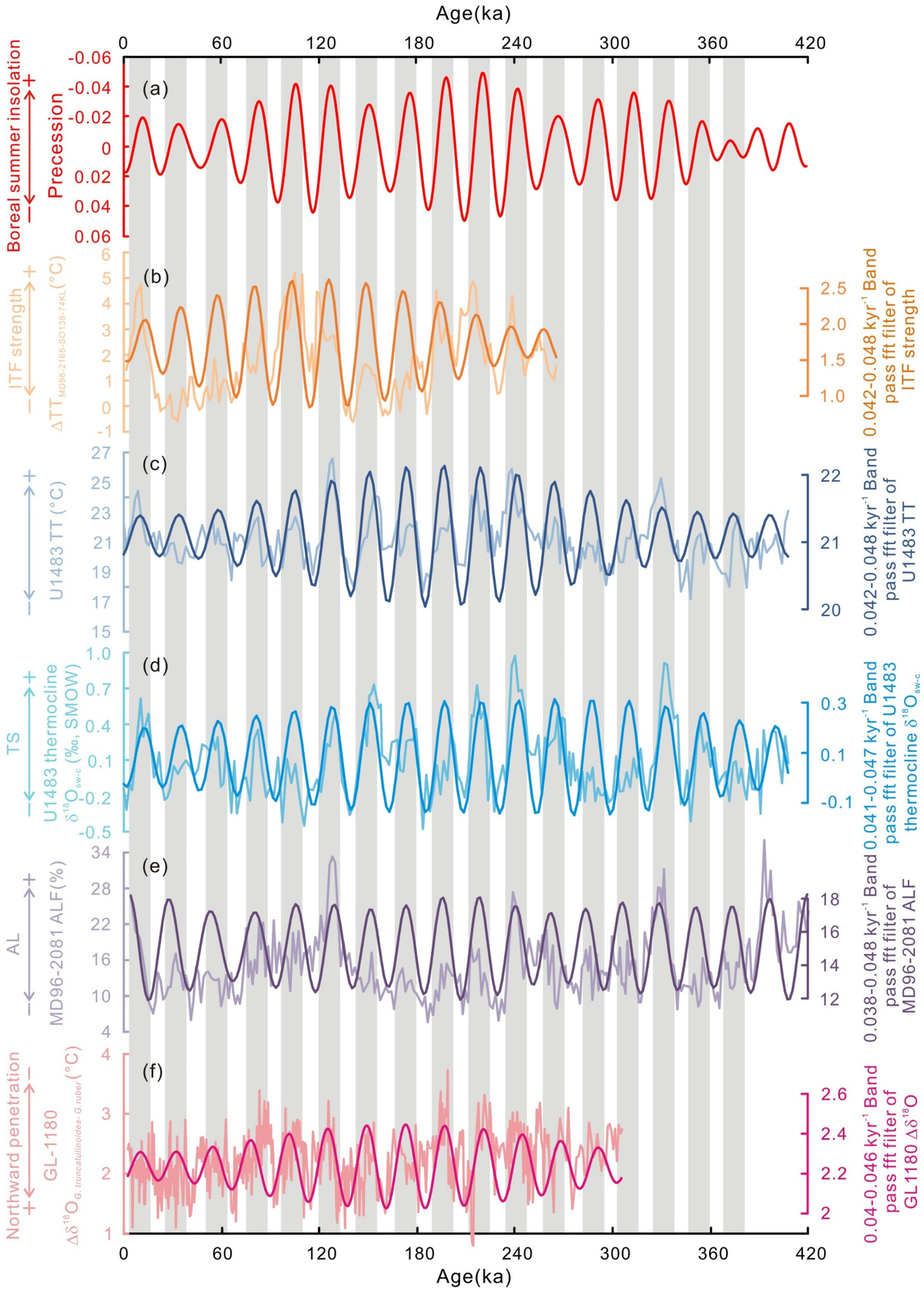

Figure 3. Comparison of variability in the temperature, salinity and strength of the ITF thermocline with the amount of the AL and northward penetration extent of SASG waters on the precession band. (a) Precessional parameter (Berger & Loutre, 1991); (b)$\Delta TT_{MD98\text{-}2165\text{-}SO139\text{-}74KL}$ as a proxy for the ITF strength (Pang et al., 2021); (c) TT and (d) TS from Site U1483 (this study); (e) ALF (%) from Core MD96-2081 as a proxy for the amount of the AL (Peeters et al., 2004); (f) $\Delta\delta^{18}O_{G.\ truncatulinoides\text{-}\ G.\ ruber}$ from Core GL-1180 as a proxy for the northward penetration extent of SASG waters (Nascimento et al., 2021). In panels (b–f), superimposed on the raw data curves are precession bandpass filtering curves.

between precession-bandpass filter of ALF (%) and precession parameter (Figures 3a and 3e). Here, we speculate that precession may influence the AL by regulating the ITF thermocline, because increased (decreased) amount of the AL and high (low) TT and TS in the South Atlantic coincide with increased (decreased) transport of the ITF thermocline and high (low) TT and TS in the Timor Sea during precession minima (maxima) (Figures 3a–3e and Figure S4 in Supporting Information S1). The results of cross-spectral analyses reinforce the perspective of the close link between the ITF thermocline and the AL, as the proxy records of which are strongly coherent on the precession band (Figure S3g in Supporting Information S1).

Modern observations revealed that waters from the ITF thermocline incorporate into the South Equatorial Current (SEC) and reach the east coast of the African continent after leaving the Timor Sea (Figure 1). Afterward, these waters flow southward into the Agulhas current (AC) through the Mozambique Channel and the east coast of the Madagascar Island and eventually join in the AL (Figure 1) (Beal et al., 2011; Gordon, 1985, 1986). Furthermore, the increased transport of the ITF thermocline will strengthen the AL (Makarim et al., 2019), which supports a previous modeling study showing that transport of the AL increases under the presence of the ITF in contrast to the scenario of a closed Indonesian seaway (Le Bars et al., 2013). Influence of the ITF on the AL is also recorded by geological archives. For instance, the weakened ITF at around 3.5–3 and 1.5 Ma was hypothesized to cause significant decrease in the AL (Petrick et al., 2018, 2019). Assuming an analogous coupling between the ITF and the AL for the last ~410 kyr, we would conclude that more (less) waters with high (low) temperature and salinity from the ITF thermocline were transport to the AL during precession minima (maxima), leading to strengthening (weakening) of the AL and high (low) TT and TS in the South Atlantic (Figures 3a–3e and 4 and Figure S4 in Supporting Information S1).

Additionally, the ALF is characterized by 10 typical tropical-subtropical planktonic foraminiferal species, which are transported from the Mozambique Channel to the AL (Peeters et al., 2004). These species could be more suitable to live in relative warm and saline waters (Bé and Hutson, 1977). Thus, increased transport of the ITF thermocline water with higher temperature and salinity would favor the ALF. It is very likely that more waters with higher temperature and salinity from the ITF thermocline passed through the Mozambique Channel and resulted in increase of ALF (%) in the AL region during precession minima (Figures 3a–3e and 4), which is clearly revealed by the significant coherence with negligible phase difference between ALF (%) and Site U1483TT and TS on the precession band (Figures S3g–S3i in Supporting Information S1). The covariance between the ITF thermocline water and ALF (%) thus provides one more line of evidence supporting our speculation that precession drove variations of the AL via regulating the ITF thermocline during the past ~410 kyr (Figure 4). Notably, some studies pointed out that the latitudinal shifts of the Southern Hemisphere subtropical front (STF) also exert the significant influencing on the AL (Biastoch et al., 2009; Mejía et al., 2014; Peeters et al., 2004). However, the latitudinal shifts of the STF on orbital timescales were dominated by obliquity and eccentricity cycles (Mejía et al., 2014; Peeters et al., 2004), thus we can exclude its implications on the AL on the precession band.

Nevertheless, a growing number of studies pointed out that the AL affected the strength and stability of the AMOC on different timescales, with increase of the AL (more saline South Atlantic thermocline water) corresponding to a stronger and more stable AMOC (e.g., Beal et al., 2011; Biastoch et al., 2008; Knorr & Lohmann, 2003; Weijer et al., 2001, 2002; Zhang et al., 2022). The increased AL during low precession would consequently indicate the concurrence of stronger and more stable AMOC. On the contrary, the deep-water formation rate in the North Atlantic is out of phase with precession, pointing to weaker AMOC during precession minima (Lisiecki, 2014; Lisiecki et al., 2008). Hence, driving of precession encounters a dilemma to account for harmonious variations between the AL and the AMOC. A recent study of Nascimento et al. (2021) suggested that the $\delta^{18}O$ difference between deep (*Globorotalia truncatulinoides*)- and surface (*Globigerinoides ruber*)-dwelling planktonic foraminiferal species ($\Delta\delta^{18}O$) from Core GL-1180 is a proxy for northward penetration extent of the South Atlantic Subtropical Gyre (SASG) water. Interestingly, the $\Delta\delta^{18}O$ is also dominated by precessional cyclicities (Figure S3f in Supporting Information S1), showing shrinkage of the SASG water during precession minima (Figure 3f, Figures S3h and S3i in Supporting Information S1) (Nascimento et al., 2021). Although the AL increased during low precession, shrinkage of the SASG water would reduce the cross-equatorial flow toward the North Atlantic and consequently lead to weakening of the AMOC (Figures 3a, 3e, 3f and 4) (Nascimento et al., 2021). Therefore, precession-driven northward penetration of the SASG may dominate over the AL to impact the strength of the AMOC.

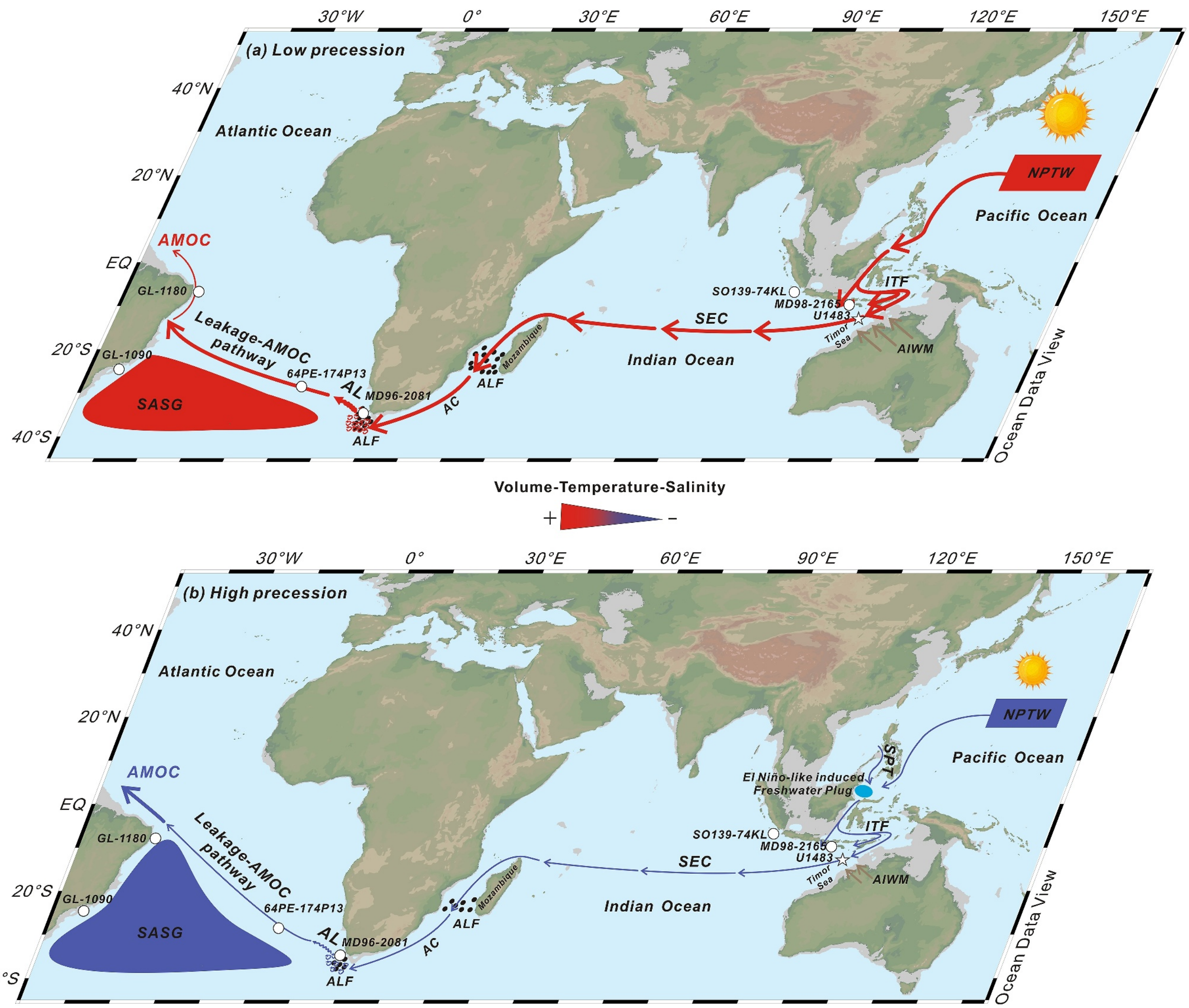

Figure 4. Sketch illustrating the relationship between the AIWM, NPTW, SPT, ITF, SEC, AC, ALF, AL, SASG and AMOC during low precession (a) and high precession (b). During low precession or high boreal summer insolation, enhanced AIWM, disappeared freshwater plug in the northern Makassar Strait under La Niña-like conditions and more NPTW forming causes increased thermocline transport and raised TT and TS of the ITF, accompanied by high ALF (%) and increased amount of the AL, further leading to raised TT and TS in the South Atlantic and more water into Leakage-AMOC pathway. However, this is not leading to strengthened AMOC due to poor northward penetration of the SASG water (a). The opposite situation occurs during high precession (b). White filled star marks Site U1483 (this study). White filled circles mark reference cores. Black dots denote the ALF (%). Gray-shaded areas denote exposed shelf areas with the sea level drop 100 m.

4. Conclusions

In this study, we reconstructed seawater temperature and salinity of the ITF thermocline in the Timor Sea over the past ~410 kyr, based on $\delta^{18}O$ and Mg/Ca of planktonic foraminiferal *P. obliquiloculata* from IODP Site U1483. By integrating our records with published paleo-oceanographic and -climatological records, we found that precession may drive transport of ITF thermocline water and as well as variations of the TT and TS through modulating the intensity of the AIWM, ENSO-like states and formation of the NPTW over the last ~410 kyr. Our investigation further revealed that precession-driven variations co-occurred in the ITF thermocline and in the AL, with large amount of the AL and warm and saline South Atlantic thermocline due to increased transport and high temperature and salinity of the ITF thermocline during low precession, and vice versa. Nevertheless, precession regulated AL variations cannot account for the strength of the AMOC, which is probably dominated by precession-driven northward penetration of the SASG water.

Data Availability Statement

Data of this manuscript are archived at Zhang (2024).

Acknowledgments

We are grateful to Dieter Garbe-Schönberg (Kiel University) for ICP-OES measurements and Nils Andersen (Leibniz Laboratory Kiel) for stable isotopes analyses. We greatly thank the International Ocean Discovery Program for providing samples. This work was supported by the National Natural Science Foundation of China (Grant 42176076 and 42376062), the National Key Research and Development Program of China (Grant 2023YFF0803900), the State Key Laboratory of Marine Geology, Tongji University (Grant MGK202402) and the Youth Innovation Team of Shaanxi Universities. We thank anonymous reviewers for constructive comments that helped us to improve the manuscript.

References

Anand, P., Elderfield, H., & Conte, M. H. (2003). Calibration of Mg/Ca thermometry in planktonic foraminifera from a sediment trap time series. *Paleoceanography*, *18*(2), 1050. https://doi.org/10.1029/2002PA000846

Ballalai, J. M., Santos, T. P., Lessa, D. V., Venancio, I. M., Chiessi, C. M., Johnstone, H. J., et al. (2019). Tracking spread of the Agulhas leakage into the western South Atlantic and its northward transmission during the last interglacial. *Paleoceanography and Paleoclimatology*, *34*(11), 1744–1760. https://doi.org/10.1029/2019PA003653

Barker, S., Greaves, M., & Elderfield, H. (2003). A study of cleaning procedures used for foraminiferal Mg/Ca paleothermometry. *Geochemistry, Geophysics, Geosystems*, *4*(9), 8407. https://doi.org/10.1029/2003GC000559

Bé, A. W., Hutson, W. H., & Be, A. W. H. (1977). Ecology of planktonic foraminifera and biogeographic patterns of life and fossil assemblages in the Indian Ocean. *Micropaleontology*, *23*(4), 369–414. https://doi.org/10.2307/1485406

Beal, L. M., Ruijter, W. P., Biastoch, A., Zahn, R., Cronin, M., Hermes, J., et al. (2011). On the role of the Agulhas system in ocean circulation and climate. *Nature*, *472*(7344), 429–436. https://doi.org/10.1038/nature09983

Bemis, B. E., Spero, H. J., Bijma, J., & Lea, D. W. (1998). Reevaluation of the oxygen isotopic composition of planktonic foraminifera: Experimental results and revised paleotemperature equations. *Paleoceanography*, *13*(2), 150–160. https://doi.org/10.1029/98PA00070

Berger, A. L., & Loutre, M. F. (1991). Insolation values for the climate of the last 10 million years. *Quaternary Science Reviews*, *10*(4), 297–317. https://doi.org/10.1016/0277-3791(91)90033-q

Biastoch, A., Böning, C. W., & Lutjeharms, J. R. (2008). Agulhas leakage dynamics affects decadal variability in Atlantic overturning circulation. *Nature*, *456*(7221), 489–492. https://doi.org/10.1038/nature07426

Biastoch, A., Böning, C. W., Schwarzkopf, F. U., & Lutjeharms, J. R. (2009). Increase in Agulhas leakage due to poleward shift of southern Hemisphere westerlies. *Nature*, *462*(7272), 497–498. https://doi.org/10.1038/nature08519

Cannon, G. A. (1966). Tropical waters in the western Pacific ocean, August-September 1957. *Deep-Sea Research and Oceanographic Abstracts*, *13*(6), 1139–1148. https://doi.org/10.1016/0011-7471(66)90705-4

Clement, A. C., & Cane, M. A. (1999). A role for the tropical Pacific coupled ocean-atmosphere system on Milankovitch and millennial time-scales. Part I: A modeling study of tropical Pacific variability. In P. U. Clark, R. S. Webb, & L. D. Keiwin (Eds.), *Mechanisms of global climate change at millennial time scales* (Vol. 112, pp. 363–371). Geophysical Monograph Series. https://doi.org/10.1029/gm112p0363

Clement, A. C., Seager, R., & Cane, M. A. (1999). Orbital controls on the El Niño/southern Oscillation and the tropical climate. *Paleoceanography*, *14*(4), 441–456. https://doi.org/10.1029/1999PA900013

Cresswell, G., Frische, A., Peterson, J., & Quadfasel, D. (1993). Circulation in the Timor Sea. *Journal of Geophysical Research*, *98*(C8), 14379–14389. https://doi.org/10.1029/93JC00317

Dang, H., Jian, Z., Bassinot, F., Qiao, P., & Cheng, X. (2012). Decoupled Holocene variability in surface and thermocline water temperatures of the Indo-Pacific warm pool. *Geophysical Research Letters*, *39*(1), L01701. https://doi.org/10.1029/2011GL050154

Donners, J., & Drijfhout, S. S. (2004). The Lagrangian view of South Atlantic interocean exchange in a global ocean model compared with inverse model results. *Journal of Physical Oceanography*, *34*(5), 1019–1035. https://doi.org/10.1175/1520-0485(2004)034<1019:TLVOSA>2.0.CO;2

Durgadoo, J. V., Rühs, S., Biastoch, A., & Böning, C. W. (2017). Indian Ocean sources of Agulhas leakage. *Journal of Geophysical Research*, *122*(4), 3481–3499. https://doi.org/10.1002/2016JC012676

Ffield, A., Vranes, K., Gordon, A. L., Susanto, R. D., & Garzoli, S. L. (2000). Temperature variability within the Makassar Strait. *Geophysical Research Letters*, *27*(2), 237–240. https://doi.org/10.1029/1999gl002377

Fine, R. A., Lukas, R., Bingham, F. M., Warner, M. J., & Gammon, R. H. (1994). The western equatorial Pacific: A water mass crossroads. *Journal of Geophysical Research*, *99*(C12), 25063–25080. https://doi.org/10.1029/94JC02277

Fine, R. A., Maillet, K. A., Sullivan, K. F., & Willey, D. A. (2001). Circulation and ventilation flux of the Pacific ocean. *Journal of Geophysical Research*, *106*(C10), 22159–22178. https://doi.org/10.1029/1999JC000184

Gordon, A. L. (1985). Indian-Atlantic transfer of thermocline water at the Agulhas retroflection. *Science*, *227*(4690), 1030–1033. https://doi.org/10.1126/science.227.4690.1030

Gordon, A. L. (1986). Interocean exchange of thermocline water. *Journal of Geophysical Research*, *91*(C4), 5037–5046. https://doi.org/10.1029/JC091iC04p05037

Gordon, A. L. (2005). Oceanography of the Indonesian seas and their throughflow. *Oceanography*, *18*(4), 14–27. https://doi.org/10.5670/oceanog.2005.01

Gordon, A. L., & Fine, R. A. (1996). Pathways of water between the Pacific and Indian oceans in the Indonesian seas. *Nature*, *379*(6561), 146–149. https://doi.org/10.1038/379146a0

Gordon, A. L., Huber, B. A., Metzger, E. J., Susanto, R. D., Hurlburt, H. E., & Adi, T. R. (2012). South China Sea throughflow impact on the Indonesian throughflow. *Geophysical Research Letters*, *39*(11), L11602. https://doi.org/10.1029/2012GL052021

Gordon, A. L., Sprintall, J., Wijffels, S., Susanto, D., Molcard, R., Van Aken, H. M., et al. (2010). Interocean exchange of thermocline water: Indonesian throughflow; "Tassie" leakage; Agulhas leakage. In J. Hall, D. E. Harrison, & D. Stammer (Eds.), *Proceedings of OceanObs'09: Sustained ocean observations and information for society* (Vol. 2, pp. 397–409). ESA Publication. https://doi.org/10.5270/OceanObs09.cwp.37

Gray, W. R., & Evans, D. (2019). Nonthermal influences on Mg/Ca in planktonic foraminifera: A review of culture studies and application to the last glacial maximum. *Paleoceanography and Paleoclimatology*, *34*(3), 306–315. https://doi.org/10.1029/2018PA003517

Greaves, M., Caillon, N., Rebaubier, H., Bartoli, G., Bohaty, S., Cacho, I., et al. (2008). Interlaboratory comparison study of calibration standards for foraminiferal Mg/Ca thermometry. *Geochemistry, Geophysics, Geosystems*, *9*(8), 1–27. https://doi.org/10.1029/2008GC001974

Haines, M. A., Fine, R. A., Luther, M. E., & Ji, Z. (1999). Particle trajectories in an Indian Ocean model and sensitivity to seasonal forcing. *Journal of Physical Oceanography*, *29*(4), 584–598. https://doi.org/10.1175/1520-0485(1999)029<0584:PTIAIO>2.0.CO;2

Holbourn, A. E., Kuhnt, W., & Xu, J. (2011). Indonesian Throughflow variability during the last 140 ka: The Timor Sea outflow. *Geological Society*, *355*(1), 283–303. https://doi.org/10.1144/SP355.14

Hut, G. (1987). *Consultants' Group Meeting on stable isotope reference samples for geochemical and hydrological investigations*. International Atomic Energy Agency (IAEA).

Jian, Z. M., Wang, Y., Dang, H. W., Mohtadi, M., Rosenthal, Y., Lea, D. W., et al. (2022). Warm pool ocean heat content regulates ocean-continent moisture transport. *Nature*, *612*(7938), 92–99. https://doi.org/10.1038/s41586-022-05302-y

Knorr, G., & Lohmann, G. (2003). Southern Ocean origin for the resumption of Atlantic thermohaline circulation during deglaciation. *Nature*, *424*(6948), 532–536. https://doi.org/10.1038/nature01855

Le Bars, D., Dijkstra, H. A., & De Ruijter, W. P. M. (2013). Impact of the Indonesian throughflow on Agulhas leakage. *Ocean Science*, *9*(5), 773–785. https://doi.org/10.5194/os-9-773-2013

Li, X., Yuan, D., Wang, Z., Li, Y., Corvianawatie, C., Surinati, D., et al. (2020). Moored observations of transport and variability of Halmahera sea currents. *Journal of Physical Oceanography*, *50*(2), 471–488. https://doi.org/10.1175/JPO-D-19-0109.1

Lisiecki, L. E. (2014). Atlantic overturning responses to obliquity and precession over the last 3 Myr. *Paleoceanography*, *29*(2), 71–86. https://doi.org/10.1002/2013PA002505

Lisiecki, L. E., Raymo, M. E., & Curry, W. B. (2008). Atlantic overturning responses to Late Pleistocene climate forcings. *Nature*, *456*(7218), 85–88. https://doi.org/10.1038/nature07425

Locarnini, R. A., Mishonov, A. V., Baranova, O. K., Reagan, J. R., Boyer, T. P., Seidov, D., et al. (2024). *World Ocean Atlas 2023, volume 2: Salinity*. In A. Mishonov Tech (Ed.), (Vol. 89, 52). NOAA Atlas NESDIS. https://doi.org/10.25923/54bh-1613

Lückge, A., Mohtadi, M., Rühlemann, C., Scheeder, G., Vink, A., Reinhardt, L., & Wiedicke, M. (2009). Monsoon versus ocean circulation controls on paleoenvironmental conditions off southern Sumatra during the past 300,000 years. *Paleoceanography*, *24*(1), PA1208. https://doi.org/10.1029/2008pa001627

Makarim, S., Sprintall, J., Liu, Z., Yu, W., Santoso, A., Yan, X., & Susanto, R. D. (2019). Previously unidentified Indonesian Throughflow pathways and freshening in the Indian Ocean during recent decades. *Scientific Reports*, *9*(1), 7364. https://doi.org/10.1038/s41598-019-43841-z

Martin, P. A., & Lea, D. W. (2002). A simple evaluation of cleaning procedures on fossil benthic foraminiferal Mg/Ca. *Geochemistry, Geophysics, Geosystems*, *3*(10), 8401–8408. https://doi.org/10.1029/2001GC000280

Mejía, L. M., Ziveri, P., Cagnetti, M., Bolton, C., Zahn, R., Marino, G., et al. (2014). Effects of midlatitude westerlies on the paleoproductivity at the Agulhas Bank slope during the penultimate glacial cycle: Evidence from coccolith Sr/Ca ratios. *Paleoceanography*, *29*(7), 697–714. https://doi.org/10.1002/2013PA002589

Mohtadi, M., Prange, M., Oppo, D. W., De Pol-Holz, R., Merkel, U., Zhang, X., et al. (2014). North Atlantic forcing of tropical Indian Ocean climate. *Nature*, *509*(7498), 76–80. https://doi.org/10.1038/nature13196

Nascimento, R. A., Venancio, I. M., Chiessi, C. M., Ballalai, J. M., Kuhnert, H., Johnstone, H. J., et al. (2021). Tropical Atlantic stratification response to late Quaternary precessional forcing. *Earth and Planetary Science Letters*, *568*, 117030. https://doi.org/10.1016/j.epsl.2021.117030

Ólafsdóttir, B. K., Schulz, M., & Mudelsee, M. (2016). REDFIT-X: Cross-spectral analysis of unevenly spaced paleoclimate time series. *Computational Geosciences*, *91*, 11–18. https://doi.org/10.1016/j.cageo.2016.03.001

Pang, X., Bassinot, F., & Sepulcre, S. (2021). Indonesian Throughflow variability over the last two glacial-interglacial cycles: Evidence from the eastern Indian Ocean. *Quaternary Science Reviews*, *256*, 106839. https://doi.org/10.1016/j.quascirev.2021.106839

Peeters, F. J., Acheson, R., Brummer, G. J., Ruijter, W. P., Schneider, R. R., Ganssen, G. M., et al. (2004). Vigorous exchange between the Indian and Atlantic oceans at the end of the past five glacial periods. *Nature*, *430*(7000), 661–665. https://doi.org/10.1038/nature02785

Peterson, R. G., & Stramma, L. (1991). Upper-level circulation in the South Atlantic ocean. *Progress in Oceanography*, *26*, 1–73. https://doi.org/10.1016/0079-6611(91)90006-8

Petrick, B., Martínez-García, A., Auer, G., Reuning, L., Auderset, A., Deik, H., et al. (2019). Glacial Indonesian throughflow weakening across the mid-pleistocene climatic transition. *Scientific Reports*, *9*(1), 1–13. https://doi.org/10.1038/S41598-019-53382-0

Petrick, B., McClymont, E. L., Littler, K., Rosell-Melé, A., Clarkson, M. O., Maslin, M., et al. (2018). Oceanographic and climatic evolution of the southeastern subtropical Atlantic over the last 3.5 Ma. *Earth and Planetary Science Letters*, *492*, 12–21. https://doi.org/10.1016/j.epsl.2018.03.054

Reagan, J. R., Seidov, D., Wang, Z., Dukhovskoy, D., Boyer, T. P., Locarnini, R. A., et al. (2024). *World Ocean Atlas 2023, volume 2: Salinity*. In A. Mishonov (Ed.) (Vol. 90, 51). NOAA Atlas NESDIS. https://doi.org/10.25923/70qt-9574

Rosenthal, Y., Boyle, E. A., & Slowey, N. C. (1997). Temperature control on the incorporation of magnesium, strontium, fluorine, and cadmium into benthic foraminiferal shells from Little Bahama Bank: Prospects for thermocline paleoceanography. *Geochimica et Cosmochimica Acta*, *61*(17), 3633–3643. https://doi.org/10.1016/S0016-7037

Rosenthal, Y., Holbourn, A. E., Kulhanek, D. K., & the Expedition 363 Scientists (2017). International Ocean Discovery Program Expedition 363 preliminary report: Western pacific warm pool. https://doi.org/10.14379/iodp.pr.363.2017

Rühs, S., Schwarzkopf, F. U., Speich, S., & Biastoch, A. (2019). Cold vs. warm water route—Sources for the upper limb of the Atlantic Meridional Overturning Circulation revisited in a high-resolution ocean model. *Ocean Science*, *15*(3), 489–512. https://doi.org/10.5194/os-15-489-2019

Ruijter, W. P., Biastoch, A., Drijfhout, S. S., Lutjeharms, J. R., Matano, R. P., Pichevin, T., et al. (1999). Indian-Atlantic interocean exchange: Dynamics, estimation and impact. *Journal of Geophysical Research*, *104*, 20885–20910. https://doi.org/10.1029/1998JC900099

Schulz, M., & Mudelsee, M. (2002). REDFIT: Estimating red-noise spectra directly from unevenly spaced paleoclimatic time series. *Computers & Geosciences*, *28*(3), 421–426. https://doi.org/10.1016/S0098-3004(01)00044-9

Shi, Z., Liu, X., & Cheng, X. (2012). Anti-phased response of northern and southern East Asian summer precipitation to ENSO modulation of orbital forcing. *Quaternary Science Reviews*, *40*, 30–38. https://doi.org/10.1016/j.quascirev.2012.02.019

Song, Q., Gordon, A. L., & Visbeck, M. (2004). Spreading of the Indonesian throughflow in the Indian ocean. *Journal of Physical Oceanography*, *34*(4), 772–792. https://doi.org/10.1175/1520-0485(2004)034<0772:SOTITI>2.0.CO;2

Spratt, R. M., & Lisiecki, L. E. (2016). A late pleistocene sea level stack. *Climate of The Past*, *12*(4), 1079–1092. https://doi.org/10.5194/cp-12-1079-2016

Sprintall, J., Wijffels, S. E., Molcard, R., & Jaya, I. (2009). Direct estimates of the Indonesian throughflow entering the Indian ocean: 2004–2006. *Journal of Geophysical Research*, *114*(C7). https://doi.org/10.1029/2008JC005257

Tsuchiya, M. (1968). *Upper waters of the intertropical Pacific ocean*. Johns Hopkins Press. 50. https://doi.org/10.4319/lo.1969.14.4.0650c

Weijer, W., Ruijter, W. P., & Dijkstra, H. A. (2001). Stability of the Atlantic overturning circulation: Competition between Bering strait freshwater flux and Agulhas heat and salt sources. *Journal of Physical Oceanography*, *31*(8), 2385–2402. https://doi.org/10.1175/1520-0485(2001)031%3C2385:SOTAOC%3E2.0.CO;2

Weijer, W., Ruijter, W. P., Sterl, A., & Drijfhout, S. S. (2002). Response of the Atlantic overturning circulation to South Atlantic sources of buoyancy. *Global and Planetary Change*, *34*(3–4), 293–311. https://doi.org/10.1016/S0921-8181(02)00121-2

Xu, J., Kuhnt, W., Holbourn, A., Regenberg, M., & Andersen, N. (2010). Indo-pacific warm pool variability during the Holocene and last glacial maximum. *Paleoceanography*, *25*(4), PA4230. https://doi.org/10.1029/2010PA001934

Zhang, P. (2024). Pulleniatina obliquiloculata stable oxygen isotope and Mg/Ca ratios record from IODP Core 363-U1483 [Dataset]. *Zenodo*. https://doi.org/10.5281/zenodo.13761597

Zhang, P., Xu, J., Beil, S., Holbourn, A., Kuhnt, W., Li, T., et al. (2021). Variability in Indonesian Throughflow upper hydrology in response to precession-induced tropical climate processes over the past 120 kyr. *Journal of Geophysical Research: Oceans*, *126*(8), e2020JC017014. https://doi.org/10.1029/2020JC017014

Zhang, P., Xu, J., Holbourn, A., Kuhnt, W., Xiong, Z., & Li, T. (2022). Obliquity induced latitudinal migration of the Intertropical Convergence Zone during the past ~410 kyr. *Geophysical Research Letters*, *49*(21), e2022GL100039. https://doi.org/10.1029/2022GL100039

Zhang, P., Xu, J., Holbourn, A. E., Kuhnt, W., Beil, S., Li, T., et al. (2020). Indo-pacific hydroclimate in response to changes of the intertropical convergence zone: Discrepancy on precession and obliquity bands over the last 410 kyr. *Journal of Geophysical Research: Atmospheres*, *125*(14). https://doi.org/10.1029/2019JD032125

Zhang, P., Xu, J., Schröder, J. F., Holbourn, A., Kuhnt, W., Kochhann, K. G. D., et al. (2018). Variability of the Indonesian throughflow thermal profile over the last 25-kyr: A perspective from the southern Makassar Strait. *Global and Planetary Change*, *169*, 214–223. https://doi.org/10.1016/j.gloplacha.2018.08.003

Zhang, P., Zuraida, R., Rosenthal, Y., Holbourn, A., Kuhnt, W., & Xu, J. (2019). Geochemical characteristics from tests of four modern planktonic foraminiferal species in the Indonesian Throughflow region and their implications. *Geoscience Frontiers*, *10*(2), 505–516. https://doi.org/10.1016/j.gsf.2018.01.011

References From the Supporting Information

Scussolini, P., Marino, G., Brummer, G.-J. A., & Peeters, F. J. C. (2015). Saline Indian Ocean waters invaded the South Atlantic thermocline during glacial termination II. *Geology*, *43*(2), 139–142. https://doi.org/10.1130/G36238.1